Korean J. Chem. Eng., **29**(9), 1187-1195 (2012)
DOI: 10.1007/s11814-011-0297-9

Preparation and characterizations of activated carbon from kenaf fiber for equilibrium adsorption studies of copper from wastewater

Zaira Zaman Chowdhury*,†, Sharifuddin Mohd. Zain*, Rashid Atta Khan*, and Md. Sakinul Islam**

*Department of Chemistry, Faculty of Science, University Malaya, Kuala Lumpur 50603, Malaysia
**Department of Chemical Engineering, Faculty of Engineering, University Malaya, Kuala Lumpur 50603, Malaysia
(*Received 10 August 2011 • accepted 15 December 2011*)

Abstract–The potential of activated carbon prepared from kenaf fiber (KF) to remove copper (II) from aqueous effluents was investigated. The fibers were first semi-carbonized, then impregnated with potassium hydroxide (KOH) and finally activated by using carbon dioxide (CO_2) gas to produce activated carbon. Pore structure and physical characteristics of the prepared kenaf fiber activated carbon (KFAC) were determined. Adsorption studies for divalent copper (Cu) ions were carried out to delineate the effect of contact time, temperature, pH and initial metal ion concentration on equilibrium adsorption capacity. The experimental data followed pseudo-second-order kinetics and Elovich Model than pseudo-first-order. Langmuir, Freundlich and Temkin models were implemented to analyze the parameters for adsorption at 30 °C, 50 °C and 70 °C. Thermodynamic parameters such as ΔG^o, ΔH^o and ΔS^o which represent Gibbs free energy, enthalpy and entropy, respectively, were evaluated. It was concluded that activated carbon from kenaf fiber (KFAC) can be used as an efficient adsorbent for removal of Cu (II) from synthetic wastewater.

Key words: Kinetics, Isotherm, Copper, Thermodynamics

INTRODUCTION

Toxic metals discharging from different industrial process effluents can cause severe contamination of ground and surface water. The careless disposal of industrial effluents contributes greatly to the poor quality of water. However, not only for rapid industrialization, deforestation and unplanned urbanization, some natural phenomena of anthropogenic activities, such as weathering of rocks and volcanic activities also play a crucial role for enriching the water reservoirs with heavy metals [1,2]. Heavy metals constitute a group of transition and post transition metals along with their metalloids, and there are about 20 heavy metals identified which are widely distributed in the environment. Unlike organic pollutants, these heavy metals are persistent in nature and do not undergo physical, chemical or microbial degradation. In addition, they have the tendency to accumulate in living organisms, having a severe impact on human health and on the sustainability of the ecosystem [3-5]. Thus, there is a growing concern about widespread contamination of water bodies by heavy metals. Extensive research has been carried out to develop innovative and promising adsorbents for treating wastewater before discharging. Various metals such as manganese (Mn), mercury (Hg), lead (Pb), cadmium (Cd), arsenic (As), copper (Cu) etc. are known to be significantly toxic due to their non-biodegradability and toxicity [6]. Among these, copper is identified as one of the most toxic metals [7]. The possible source of copper in industrial effluents includes paper and pulp, fertilizer, wood preservatives, refineries, metal cleaning and plating bath [8]. The excessive ingestion of copper above the required limit may cause renal and hepatic damage, severe mucosal irritation, widespread capillary damage, gastrointestinal irritation and possibly necrotic changes in kidney and liver. According to the World Health Organization (WHO), maximum acceptable limit for Cu (II) concentration in drinking water should be 1.5 mg/*l*. As a result, it is essential that the filtered water should be given some treatment before domestic supply.

The ultimate goal of this endeavor is to identify a low cost, effective adsorbent for removal of heavy metals including copper from aqueous streams. In this regard, a variety of methods including precipitation, coagulation, ion exchange, membrane processes and electrolytic technologies are frequently employed to remove copper along with some other heavy metals in single or binary solute systems [9-12]. However, these conventional methods have certain major disadvantages such as incomplete removal, high operating cost, and production of toxic sludge which requires further processing or careful disposal. Among these, adsorption onto commercial activated carbon is a well established and effective technique. But it is highly expensive as it is mostly produced from non renewable sources of coal, lignite, peat etc. However, elimination of heavy metals ions, as well as copper from aqueous effluents by using agro-based by products has received much attention recently [13]. Several adsorbents derived from low cost materials such as grape stalk [14], black gram husk [15], olive stone [16], blast furnace sludge [17], sewage sludge ash [18], paper mill sludge [19], herbaceous peat [20], activated carbon [21,22], oil palm ash [23] etc., for purification of Cu (II) rich effluents have been reported in literature.

The present research explores the suitability of kenaf fiber based activated carbon (KFAC) as an adsorbent for removal of copper from synthetic wastewater. Kenaf (*Hibiscus cannabinus* L.) has same types of morphological features like cotton and jute and is presently grown in Malaysia abundantly. In Malaysia, the National Kenaf Research and Development Program has been started to produce kenaf due to its prolonged application in different manufacturing

†To whom correspondence should be addressed.
E-mail: zaira.chowdhury76@gmail.com

sectors. The government has allocated around 12 million RM [24] for further development of the kenaf-based industry under the 9th Malaysia Plan (2006-2010). This research aims to determine the adsorption mechanisms including reaction kinetics, isotherm studies and evaluation of thermodynamic parameters for the sorption process of Cu (II) cations onto KFAC.

EXPERIMENTAL

1. Preparation of Stock Solution

All reagents and chemicals used for the research were analytical grade chemicals. Stock solution of Copper (II) having concentration of 1,000 mg/*l* was prepared by dissolving definite amount of $CuSO_4 \cdot 5H_2O$ using double distilled water. Various test solutions of Cu (II) ranging from 50 mg/*l* to 100 mg/*l* were prepared by subsequent dilution of the stock solution. The initial pH was adjusted to 5.5 using a pH meter (Mettles Toledo, Model: Ross FE 20, USA) for kinetics study. Fresh dilution of the stock solution was done before each adsorption study.

2. Preparation of Activated Carbon (KFAC)

Kenaf fibers (KF) used in this research were obtained from MARDI (Malaysian Agricultural Research and Development Institute). Preliminary washing of the fibers with hot distilled water was done to remove dust-like impurities and inorganic matters onto their surfaces. It was dried at 105 °C for 24 hours to remove all moisture. The dried samples were cut into small pieces, sieved to the size of 1-2 mm. and stored in air-tight containers to prevent moisture build up and fungi infections. 40 gm of dried fiber samples were placed on the metal mesh located at the bottom of the tubular reactor under 150 cm^3/min flow rate of purified nitrogen gas for semi carbonization. At this stage, the heating rate was kept constant at 10 °C/min. The temperature was increased from room temperature to 400 °C and kept constant for 2 hours. After semi carbonization, the char was allowed to cool at room temperature under nitrogen flow at the same flow rate and stored in air-tight containers. The char and KOH ratio was maintained at 1 : 4. A definite amount of KOH pellets were mixed together with 40 gm of char and 250 ml deionized water was added slowly in a 500 ml beaker. The mixture was stirred occasionally to dissolve all fragments of KOH pellets. The beaker containing char mixed with KOH and water was placed inside an oven overnight at 105 °C for dehydration. After the water is completely evaporated, it will leave behind only KOH onto the fiber sample. The impregnation ratio was calculated by using Eq. (1):

$$\text{Impregnation ratio (IR)} = \frac{W_{KOH}}{W_{Char}} \quad (1)$$

Here, W_{KOH}=the dry weight of potassium hydroxide pellets and
W_{char}=the dry weight of char.

Precisely weighted amount of KOH impregnated chars was placed inside the tubular furnace while keeping the nitrogen gas flow rate about 150 cm^3/min and heating rate about 10 °C/min constant. The temperature was increased from room temperature to 500 °C. After the activation temperature of 500 °C was reached, the gas flow was changed to carbon dioxide at the same flow rate and kept constant for 1.25 hour. The prepared activated carbon was cooled to room temperature under the same flow rate of nitrogen gas mentioned above. Then the final product obtained from the furnace was washed with hot deionized water for several times to remove residual KOH. During the washing process, 0.1 M hydrochloric acid (HCl) was used until the pH of the washing solution reached to 6-7. The washed samples of activated carbon were dried at 105 °C in an oven until completely dried. They were stored in air-tight container for adsorption study.

3. Physiochemical Characterization of KFAC

A scanning electron microscope, SEM (Model Leo Supra 50VP Field Emission, UK), was used to study the porous texture of KFAC. Surface area, pore volume and pore diameter of the prepared activated carbon fiber were measured by Autosorb1, Quantachrome Autosorb Automated gas sorption system supplied by Quantachrome. Before the nitrogen gas adsorption was performed, the activated carbon fiber was outgassed under vacuum at temperature 300 °C for 4 hours to remove any moisture content from its surface. Surface area and pore volume were calculated by Brunauer Emmett Teller (BET). Above-mentioned procedure with necessary calculation was automatically performed by software (Micropore version 2.26) available with the instrument. The surface functional groups of the KFAC were detected by Fourier transform infrared (FTIR) spectroscope (FTIR-2000, PerkinElmer). The spectra were recorded from 4,000 to 400 cm^{-1}. The average bulk density was determined by water displacement of a specific amount of prepared KFAC.

4. Equilibrium Adsorption Studies

0.2 gm of prepared KFAC was added with 50 ml of different concentration of Cu (II) solution at 150 rpm. The remaining concentration of Cu (II) was analyzed after predetermined interval of time until the system reached equilibrium by using atomic absorption spectrophotometer (Perkin - Elmer Model 3100). Effect of pH was studied by varying the pH of the solution from 2-12, keeping other parameters of adsorbent dose, agitation speed and volume of solution constant.

5. Isotherm Studies

For isotherm studies, each experiment was carried out at 30 °C in a thermoregulated water bath (Haake Wia Model, Japan) shaker with cover to prevent heat loss to the surroundings. The equilibrium adsorption amount (q_e) was calculated using Eq. (2):

$$q_e = \frac{(C_i - C_e)}{W} V \quad (2)$$

Here, q_e=the adsorption amount of metal ion (mg/g) at equilibrium contact time,
W=the weight of adsorbent (g), and
V=the volume of solution (ml).
C_i=initial concentration
C_e=final concentration

The removal efficiency of the metal ion was calculated by using Eq. (3):

$$\text{Removal}\% = \frac{C_i - C_e}{C_i} \times 100 \quad (3)$$

RESULTS AND DISCUSSION

1. Surface Characterization of KFAC

The FTIR spectrum is an essential tool to identify the surface

Table 1. Analysis of FTIR spectra of KFAC before and after adsorption of Cu (II) ions

IR peak	Frequency (cm^{-1})		Peak
	Before adsorption	After adsorption	Assignment
1	615.74	617.47	C-H out-of-plane bending of benzene derivatives
2	838.40, 876.63	-	C-H out-of-plane deformation
3	1116.45	1114.56	-CO stretching for secondary alcohol
4	1384.82	-	C-H bending of -CH_3 group
5	-	1569.87	C=O stretching for carboxylate anions, (-COOH) group
6	1627.57	-	C=O stretching for carboxylate anions, (-COOH)
7	2359.86	2368.11	More strongly hydrogen bonded -OH group
8	3414.53	3366.68	Intra and intermolecular hydrogen bonded -OH stretching vibration

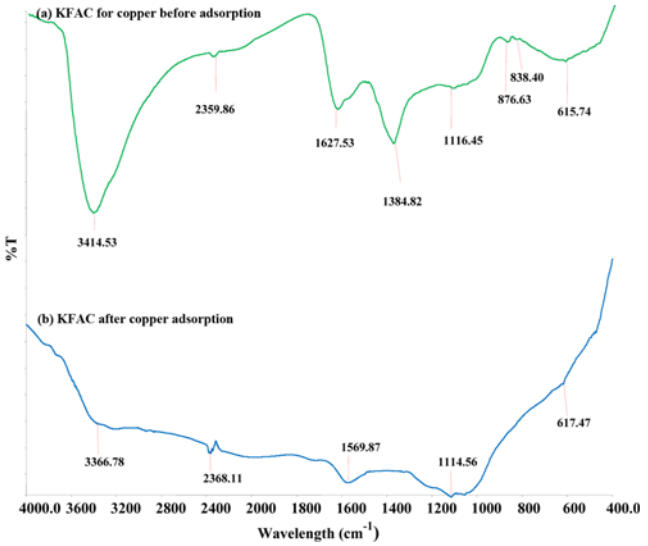

Fig. 1. FTIR spectra of kenaf fiber based activated carbon (KFAC) (a) before and (b) after adsorption of Cu (II) from aqueous solution.

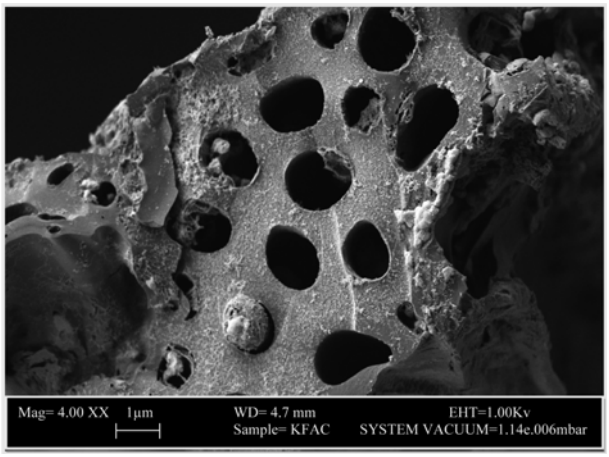

Fig. 2. SEM image of KFAC prepared for Cu (II) adsorption.

functional groups which can contribute extensively to enhance adsoption effeciency of the activated carbon for divalent cations by surface complexation. The major peaks recorded for KFAC before and after adsorption are listed in Table 1. Fig. 1 shows that many functional groups shifted to different frequency level or disappeared after adsorption, indicating the possible involvement of those groups for uptake of Cu (II) cations. It can be observed that the sharp and intense peak at around 3,414.53 cm^{-1} was shifted to a lower frequency level of 3,366.78 cm^{-1} and after adsorption it was broad and its intensity became less also. These above-mentioned peaks correspond to the -OH stretching vibration due to inter- and intramolecular hydrogen bonding of polymeric compounds such as phenols, alcohols and carboxilic acids. The minor peak of 2,359.86 cm^{-1} before adsorption shifted to a higher frequency level of 2,368.11 cm^{-1} after adsorption, which represented that the hydrogen bonded -OH group was involved for binding Cu (II) from synthetic wastewater. The peaks at 1,627.53 cm^{-1} and 1,569.87 cm^{-1} in both the spectra were due to symmetric stretching vibration of C=O in carboxylic acid group (-COOH). The minor peaks at around 838.40 cm^{-1} and 876.63 cm^{-1} correspond to -C-H bending vibration which disappeard after adsorption. However, the minor peak of 615.74 cm^{-1} shifted to slightly higher wave number of 617.47 after adsorption.

The porous structure of KFAC sample obtained from SEM image is shown by Fig. 2. It is clear that a significant number of pores with different structure were formed due to physiochemical activation of the raw fiber. It shows that the physiochemical activation process by using KOH and CO_2 was successful in creating well-developed pores on the surfaces having finely defined walls surrounding the pores. However, semi carbonization step was necessary to break down the cellulosic linkage of the precursor. This would ensure more diffusion of KOH and CO_2. At higher temperature, the reaction between C-KOH would occur spontaneously in presence of CO_2 gas. Thus it would enhance the surface area by creating new pores inside the carbon matrix of the char. The SEM micrograph indicated that the pores were made up of cylinder-like tubes which would easily capture and retain Cu (II) ions from aqueous solution. Similar results were reported by previous researchers for preparation of activated carbons derived from pistachio-nut shells, jute and coconut fiber [25,26].

The physiochemical characterization of the prepared activated carbon is listed in Table 2. According to the International Union of Pure and Applied Chemistry (IUPAC 1972) classification, pores can be categorized into three main groups depending on pore diameters: micropores (pore size<2 °A), mesopores (pore size 2-50 °A) and macropores (pore size>50 °A) [27]. Here, the activated carbon prepared had the average pore diameter of 22.9 °A. Therefore, it was concluded that, KFAC can be classified as mesoporous type

Table 2. Physio-chemical characteristics of KFAC for sorption of Cu (II) ions

Physio-chemical characteristics	Values
BET surface area	330.4023 m^2/g
Langmuir surface area	557.80 m^2/g
Micropore surface area	361.3 m^2/g
Total pore volume	0.189 cm^3/g
Average pore diameter	22.9 °A
Cumulative adsorption surface area (BJH method)	178.3 m^2/g
T-method for micro-pore surface area	180.2 m^2/g
Bulk density	0.353 g/ml
pH_{ZPC}	6.58

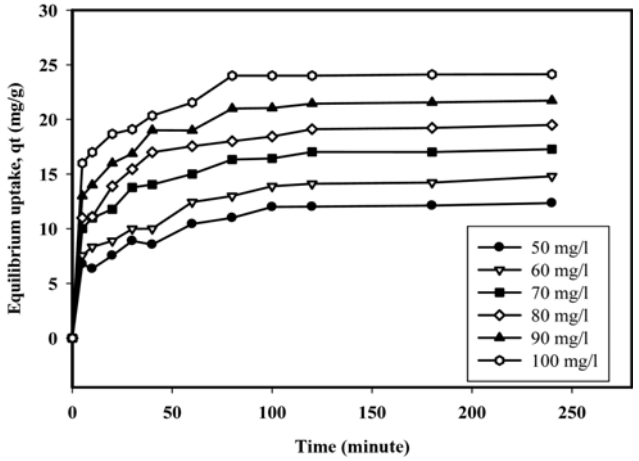

Fig. 3. Effect of initial metal ion concentration on equilibrium uptake (mg/g) of Cu (II) cation from solution at 30 °C temperature.

activated carbon.

2. Equilibrium Adsorption Studies

Fig. 3 depicts the effect of initial Cu (II) ion concentration and uptake with equilibrium contact time. It can be observed from the graph that the amount of uptake q_t (mg/gm) increased with increasing agitation time, and after certain period of time it reached a constant value, which reflects that the system had reached equilibrium. The adsorption was rapid at initial stage of contact period; after that when it was approaching towards the equilibrium time, it became relatively slower. The rate of uptake was initially high due to the availability of larger surface area of the prepared activated carbon fiber. During the initial stage of adsorption, a large number of vacant sites were available to capture copper ions. After lapse of some time, the surface adsorption sites were already occupied by the cations of copper. The remaining vacant sites were difficult to capture by residual Cu (II) ions due to the presence of repulsive forces between the cations adsorbed on the solid surface of the activated carbon and the cations present in liquid phase dissolved in the solution. The trend of the line graph showed that as the concentration of the cation was increased from 50 mg/*l* to 100 mg/*l*, the sorption capacity by the prepared activated carbon was also increased. The plot reflects that equilibrium time of 100 min. was required for all the concentration to reach equilibrium and after that the adsorption did not change

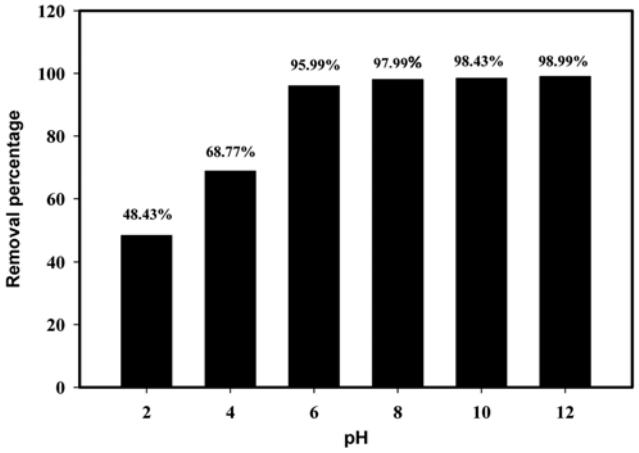

Fig. 4. Effect of pH on of equilibrium uptake (mg/g) of Cu (II) cations from solution at 30 °C temperature.

significantly. The experimental data were measured for 240 minutes to ensure that full equilibrium was attained.

3. Effects of pH on Removal Percentage

To obtain optimum pH range on uptake, the solution pH was varied from 2-12, while the other variable constant was kept constant. The graph in Fig. 4 shows the effect of pH on removal percentage of Cu (II) by KFAC. At pH 2, a higher concentration of H^+ ions in the solution competes with Cu^{2+} for the adsorption sites resulting less removal percentage. Thus the adsorption was reasonably low around 48.43% at pH 2. Similar observation had been reported for Cd^{2+} and Zn^{2+} adsorption on rice husk ash [28]. At pH 6, there are three main species of copper present in solution [29]. These species could interact with the surface hydroxide (-OH) groups and be adsorbed by the following two mechanisms of ion exchange and hydrogen bonding resulting greater removal efficiency.

(a) Ion Exchange:

$$(-RO^{+}H_2)+Cu^{2+} \longrightarrow (RO)\,Cu+2H^{+} \quad (I)$$

$$(-RO^{+}H_2)+Cu\,(OH)^{+} \longrightarrow (-RO)\,CuOH+2H^{+} \quad (II)$$

(b) Hydrogen Bonding:

$$2(\text{--R-OH})+Cu\,(OH)_2 \longrightarrow (\text{-R-OH})_2 \text{ ----- } Cu(OH)_2 \quad (III)$$

Similar observation had been reported for Cu^{2+} adsorption orange peel, saw dust and bagasse [30]. In addition, carboxylic groups (-COOH) also took part in adsorption. It is well known that the carboxylic groups present on the surface of the activated carbon have pKa values from 3 to 5. Therefore, at higher pH of 6, the acidic group started to dissociate. Thus, more interactions between negatively charged carboxylate ions and positively charged Cu^{2+} ions occurred which resulted in more removal efficiency.

$$(c)\ nR\text{-}COOH+Cu^{2+} \longrightarrow (R\text{-}COO)_n\,Cu+nH^{+} \quad (IV)$$

Here, R represents carbon matrix. Cu^{2+} belongs to transition metals having empty d-orbital that can be occupied easily by lone pair of electrons of oxygen in -COOH and -OH of the activated carbon surface to form stable complexes. Thus, it can be postulated that the adsorption process of Cu^{2+} can undergo by ion exchange, hydrogen bonding and surface complexation by the prepared activated carbon.

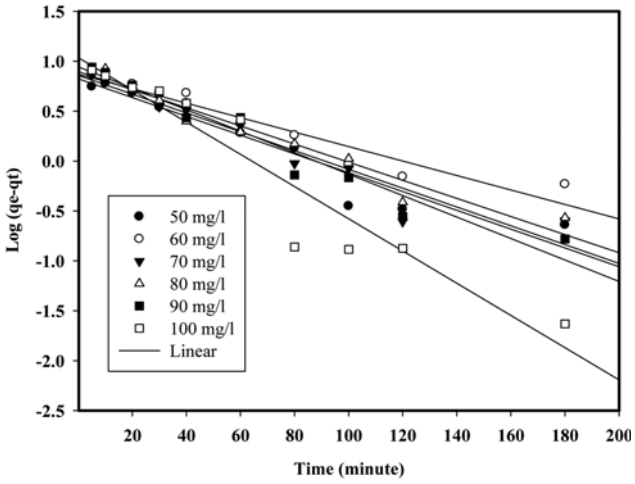

Fig. 5. Pseudo-first order kinetics for adsorption of Cu (II) cation onto KFAC at 30 °C temperature.

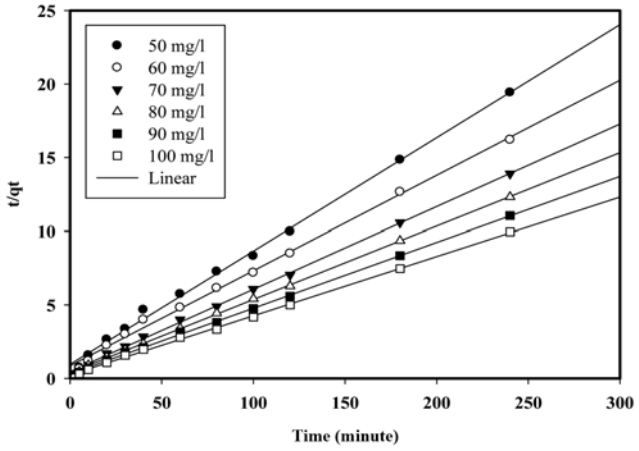

Fig. 6. Pseudo-second order kinetics for adsorption of Cu (II) cation onto KFAC at 30 °C temperature.

However, it is well known that at basic pH heavy metals like Cu (II) start to precipitate. Therefore, to avoid cooperative effects of adsorption and precipitation, all the batch experiments were conducted in slightly acidic medium of pH 5.5.

4. Equilibrium Kinetic Modeling

To estimate the kinetic parameters, pseudo-first-order and pseudo-second-order models were implemented to analyze the experimental data.

The linear form of pseudo-first-order equation [31-33] can be expressed as:

$$\log(q_e - q_t) = \log q_e - \frac{K_1}{2.303}t \tag{4}$$

$$h = K_1 q_{e\,cal} \tag{5}$$

Here, q_e and q_t denote the amount of adsorbed (mg/g) at equilibrium and at any time t, K_1 is the first-order rate constant (min^{-1}) and h (mg/g-min^{-1}) is the initial rate of sorption. From the plots of log ($q_e - q_t$) versus t (min) as shown by Fig. 5, K_1 can be calculated from the slope and theoretical q_e (mg/g) can be obtained from intercepts. The differential equation of pseudo-second order can be given by:

$$\frac{dq_t}{dt} = K(q_e - q_t)^2 \tag{6}$$

Integrating this for the boundary conditions t=0 to t and q_t=0 to q_t, gives:

$$\frac{t}{q_t} = \frac{1}{K_2 q_e^2} + \frac{1}{q_e}t \tag{7}$$

$$h = K_2 q_{e\,cal}^2 \tag{8}$$

Here, K_2 is the rate constant of second-order adsorption and h (mg/g-min^{-1}) is the initial rate of sorption. The linear plots of t/q_t versus t determine $1/q_e$ as slope and $1/K_2 q_e^2$ as intercepts. The linear plots of pseudo-second order model is shown in Fig. 6 and the model parameters are listed in Table 3.

According to intra-particle diffusion the uptake varies almost proportionally with the half power of time, $t^{0.5}$ [34]. The prediction of the rate-limiting step is essential to have insight about the adsorption mechanism. The intraparticle diffusion coefficient K_{id} can be calculated by Eq. (9):

$$q_t = K_{id} t^{0.5} \tag{9}$$

The linear plots of q_t versus $t^{0.5}$ are shown by Fig. 7. The slope of the plot has been defined to give the intraparticle diffusion parameter K_{id} (mg/g-hour$^{0.5}$). The intercept of the plot reveals C, the boundary layer effect. It is assumed that the larger the intercept, the greater the contribution of the surface sorption in the rate-controlling step. The calculated intraparticle diffusion coefficient K_{id} values are listed in Table 4.

The experimental data were further analyzed by using the Elovich equation which provides the insight about the chemisorption nature of the system under investigation [35]. The following equa-

Table 3. Comparison of pseudo-first order and pseudo-second order adsorption rate constant for different initial concentration at 30 °C temperature

	Pseudo first order					Pseudo second order			
C_0 (mg/*l*)	$q_{e,(exp)}$ (mg/g)	$q_{e,(cal)}$ (mg/g)	K_1 (min^{-1})	h	R^2	$q_{e,(cal)}$ (mg/g)	K_2 (min^{-1})	h	R^2
50	12.353	11.0918	0.05066	0.562	0.982	13.1578	0.00593	1.03	0.996
60	14.810	8.27942	0.02764	0.228	0.965	15.6250	0.00475	1.16	0.996
70	17.278	11.8304	0.04836	0.572	0.980	18.5185	0.00544	1.87	0.998
80	19.499	8.26040	0.02764	0.228	0.982	20.0000	0.00665	2.66	0.999
90	21.724	8.87156	0.04836	0.429	0.952	22.7273	0.00607	3.14	0.999
100	24.137	10.6905	0.03455	0.339	0.954	26.3157	0.00464	3.21	0.998

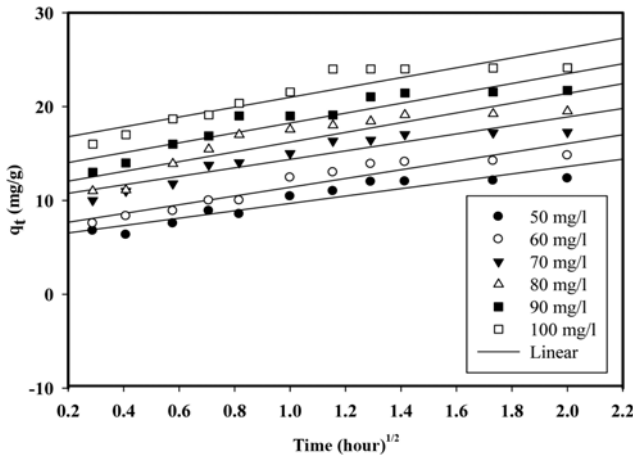

Fig. 7. Intra-particle diffusion rate studies for adsorption of Cu (II) cation onto KFAC at 30 °C temperature.

Table 4. Intra particle diffusion parameter at différent initial concentration at 30 °C temperature

Initial concentration (mg/L)	C	K_{dif} (mg/gh$^{0.5}$)	R^2	$q_{e,cal}$ (mg/g)
50	5.716	3.970	0.889	13.656
60	6.660	4.808	0.907	16.276
70	9.682	4.753	0.904	19.188
80	11.04	5.154	0.808	21.348
90	12.94	5.307	0.864	23.554
100	15.29	5.815	0.917	26.920

tion is used to calculate the model parameters:

$$q_t = \frac{1}{b}\mathrm{Ln}(ab) + \frac{1}{b}\mathrm{Ln}t \quad (10)$$

Here, a (mg/g-h) is the initial sorption rate; b (g/mg) represents activation energy and extent of surface coverage for chemisorption. The value of 1/b Ln (ab) is the sorption quantity when t (time) equals to zero, that is, t is 1 hour; whereas 1/b is indicative of the number of sorption sites for binding. The linear plots of the Elovich model are shown by Fig. 8 and the model parameters are listed in Table 5.

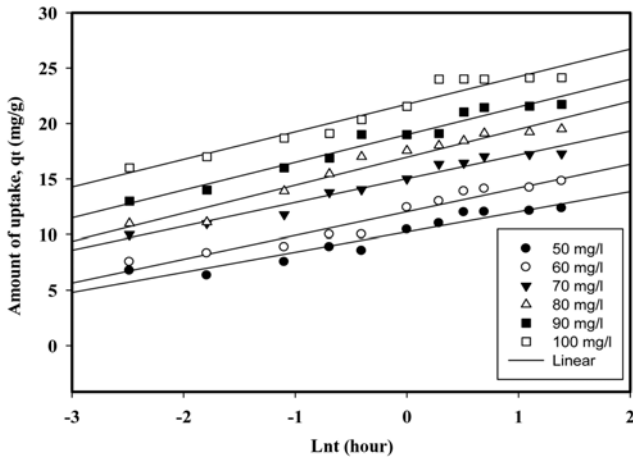

Fig. 8. Elovich equation for adsorption of Cu (II) cation onto KFAC at 30 °C temperature.

Table 5. Elovich model for kinetics study of Cu (II) onto KFAC at 30 °C temperature

Initial concentration (mg/L)	1/b	1/b ln (ab)	R^2	$q_{e,cal}$ (mg/g)
50	1.821	10.24	0.925	12.764
60	2.195	12.13	0.935	15.173
70	2.220	15.10	0.976	18.178
80	2.508	16.95	0.946	20.427
90	2.516	19.01	0.964	22.498
100	2.683	21.92	0.966	25.639

The correlation coefficient R^2 of pseudo-first-order kinetics was 0.95 to 0.98 for all the concentration range being studied, reflecting physisorption nature of KFAC towards Cu (II) cation up to a certain extent. The calculated q_e (mg/g) values obtained from pseudo-first-order kinetics did not agree well with the experimental q_e (mg/g) values. From Fig. 5, it was observed that the first-order kinetics fits well for initial 40 minutes and after that the experimental data deviates from the theory. Similar trend was reported for adsorption of dyes on peat particles, and it was concluded that the first-order model was only suitable for initial rapid stage of sorption [36]. Thus, it can be concluded that it is not appropriate to use the pseudo-first-order kinetic model to predict the adsorption kinetics for Cu (II) onto KFAC for the entire adsorption period.

On the contrary, the correlation coefficient R^2 for the second-order kinetic model was almost equal to unity for all the concentrations, signifying the applicability of the model. Moreover, the calculated q_e (mg/g) values obtained from pseudo-second-order kinetics were in good agreement with the experimental q_e (mg/g) values. Thus, it appeared that the system under study is more suitably described by pseudo-second-order kinetics which was based on the assumption that the rate-limiting step may be chemisorptions concerning valency forces through sharing and exchange of electrons. The Elovich model gave a better fit than the pseudo-first-order model, which further confirms the chemisorption nature of Cu (II) onto prepared activated carbon.

The plots of intra-particle diffusion showed that the lines did not pass through the origin. This implied that the rate-limiting process is not only governed by intraparticle diffusion. Some other mechanism along with intraparticle diffusion was involved for the entire adsorption process [37]. It was found that K_{id} values increased with the increasing initial concentrations of Cu (II) solution. This was due to the greater driving force at higher concentration range.

5. Equilibrium Isotherm Studies

Isotherm studies are essential to interpret the experimental data for adsorption process effectively. The most commonly used isotherm models for heavy metal sorption are the Langmuir, Freundlich, and Temkin isotherms.

The Langmuir isotherm deals with the maximum monolayer adsorption capacity of the sorbent under definite condition, and it assumes constant heat of adsorption for all the active binding sites

present on the adsorbent [38]. It is expressed by the following equation:

$$q_e = \frac{K_L C_e}{1 + q_L C_e} \quad (12)$$

The linear form of the Langmuir isotherm can be given by:

$$\frac{C_e}{q_e} = \frac{1}{q_{max} K_L} + \frac{1}{q_{max}} C_e \quad (13)$$

Where, q_e is related to the retention capacity of the cation (mg/g) at equilibrium time, C_e is the equilibrium cation concentration in liquid phase (mg/*l*), q_{max} reflects the maximum monolayer adsorption capacity of the adsorbent (mg/g), and K_L is the Langmuir adsorption constant (*l*/mg) related to the binding energy between the adsorbent and adsorbate. When C_e/q_e is plotted against C_e, a straight line with slope $1/q_{max}$ and intercept of $1/q_{max}K_L$ is obtained.

The essential characteristics of the Langmuir equation can be expressed in terms of a dimensionless factor, R_L which is given below:

$$R_L = \frac{1}{1 + K_L C_o} \quad (14)$$

C_o is the highest initial cation concentration (mg/*l*) used for the study. The values of separation factor R_L, can be summarized:

Value of R_L	Types of isotherm
$R_L > 1$	Unfavorable
$R_L = 1$	Linear
$0 < R_L < 1$	Favorable
$R_L = 0$	Irreversible

The linear plot of Langmuir Isotherm at 30 °C temperature is presented by Fig. 9.

The Freundlich isotherm gives the relationship between equilibrium uptake and concentration based on the multilayer adsorption properties of the adsorbent. According to Freundlich isotherm, the adsorbent surface is heterogeneous. This isotherm is derived from the assumption that the adsorption sites are distributed exponentially with respect to the heat of adsorption [39]. It is expressed by:

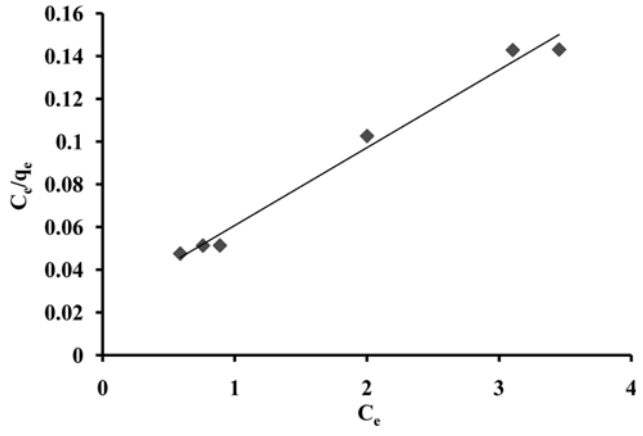

Fig. 9. Langmuir isotherm for adsorption of Cu (II) cation onto KFAC at 30 °C temperature.

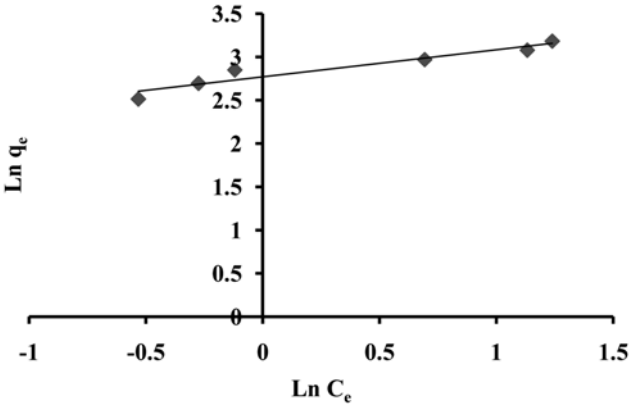

Fig. 10. Freundlich isotherm for adsorption of Cu (II) cation onto KFAC at 30 °C temperature.

$$q_e = K_f C_e^{1/n} \quad (15)$$

The linear form of Freundlich isotherm is:

$$\ln q_e = \ln K_f + \frac{1}{n} \ln C_e \quad (16)$$

Here, K_f (mg/g) and 1/n represent the affinity of the adsorbate towards the adsorbent and intensity of adsorption, respectively. Fig. 10 displays the linear plot of Freundlich Isotherm at 30 °C temperature.

According to the Temkin isotherm, the effects of the heat of adsorption of all molecules in the layer would decline linearly with coverage due to the adsorbate and adsorbent interactions [40]:

$$q_e = \frac{RT}{b} \ln K_T C_e \quad (17)$$

Eq. (17) can be linearized as:

$$q_e = \frac{RT}{b} \ln K_T + \frac{RT}{b} \ln C_e \quad (18)$$

Here, RT/b=B (j/mol), which is the Temkin constant related to heat of sorption, whereas K_T (L/g) represents the equilibrium binding constant corresponding to the maximum binding energy. R (8.314 J/mol k) is universal gas constant and T °K is absolute solution temperature.

However, the present investigation was carried out to analyze the above-mentioned isotherm parameters at 30 °C, 50 °C and 70 °C, and the model parameters are listed in Table 6. The higher correlation coefficient of the Langmuir model recommended that the adsorption process was monolayer [41] and adsorption of each adsorbate had equal activation energy for the binding sites. The separation factor, R_L value determined was less than 1, indicating that the adsorption of Cu (II) onto KFAC is favorable. The Langmuir model was found to fit the data significantly better than the Freundlich model, which showed the more homogeneous nature of KFAC. Freundlich exponent, 1/n, ranging between 0 and 1, is a measure of adsorption intensity or surface heterogeneity. The involvement of non-identical groups for adsorption mechanism also suggested surface heterogeneity of the prepared activated carbon. Similar observation had been reported for Cu (II) adsorption on prunus amygdalus shell [42]. A value of 1/n below one reflects favorable adsorption of Cu (II) onto

Table 6. Isotherm model parameters at 30 °C, 50 °C and 70 °C temperature

Temp. (°C)	Langmuir isotherm				Freundlich isotherm			Temkin isotherm		
	q_{max} (mg/g)	K_L (*l*/mg)	R_L	R^2	K_F (mg/g) (*l*/mg)$^{1/n}$	1/n	R^2	B	K_T (*l*/mg)	R^2
30	27.78	1.499	0.0066	0.986	15.95	0.312	0.919	5.564	18.75	0.938
50	29.42	1.545	0.0064	0.985	16.78	0.340	0.910	6.112	16.67	0.937
70	30.30	1.834	0.0054	0.911	18.44	0.464	0.899	8.121	10.28	0.864

Table 7. Thermodynamic parameters of Cu (II) sorption onto KFAC

Temperature, °K	ΔG^o (kj-mol^{-1})	ΔH^o (kj-mol^{-1})	ΔS^o (jK^{-1} mol^{-1})
303	1.019	4.281	0.0173
323	1.168		
343	1.728		

KFAC. Evaluation of Temkin model parameters with high correlation coefficient clearly reflects the strong affinity of Cu (II) onto KFAC.

6. Effect of Temperature and Thermodynamics Characterizations

The thermodynamic parameters related to ΔG^o, Gibbs free energy, ΔH^o, change in enthalpy of reaction and ΔS^o, change in entropy of adsorbate-adsorbent reaction [43] can be calculated by using the following equations:

$$\ln K_L = \frac{\Delta S}{R} + \frac{\Delta H}{RT} \quad (19)$$

$$\Delta G = RT \ln K_L \quad (20)$$

Here, K_L (*l*/mg) is the Langmuir Isotherm constant at different temperature; R is universal gas constant (8.314 j/mol·K) and T is absolute temperature in Kelvin. The values of ΔH^o and ΔS^o can be determined from the graph of ln K_L versus 1/T. The calculated values of thermodynamic parameters are listed in Table 5. The enthalpy change obtained here is 4.281 (Kj-mol^{-1}), which is positive reflecting endothermic nature of sorption. The result is consistent with successive increase of Langmuir maximum monolayer capacity, q_m (mg/g) and Freundlich affinity factor, K_F with the increase of temperature. This reflects the fact that higher temperature ensures more removal percentage of Cu (II) from synthetic wastewater. The positive value of entropy, ΔS^o, represents an increase in the degree of freedom of the adsorbate. The positive value of ΔS^o also reflects that some changes occur in the internal structure of KFAC during the adsorption process. Similar types of observation were reported previously for removal of lead from wastewater by using activated palm ash [42]. The magnitude of Gibbs free energy change, ΔG^o, obtained is positive demonstrating that the adsorption took place but nonspontaneously for the temperature range being studied here. Similar observation had been reported for adsorption of Cd (II) expanded perlite [44] and Ni (II) by hazelnut shell [45] and expanded perlite [44], Cr (VI) by pine needles, almond shell and cactus [45].

CONCLUSION

The present study aimed to prepare, characterize and evaluate the application of activated carbon derived from kenaf fiber (KFAC) to remove copper (II) from synthetic wastewater. Results obtained indicate that a very fast and efficient removal of copper ions can be achieved by using KFAC. Experiments were conducted with less amount of activated carbon to solution (0.2 g/50 ml solution) ratio, aiming to understand the reaction kinetics, the effect of pH and temperature. In this regard, thermodynamic parameters were determined and the adsorption of copper ions onto KFAC was found to be endothermic. An increase in temperature resulted in higher loading per unit weight of the adsorbent. The research indicates that the findings will be obliging up to a great extent for treating Cu (II) contaminated effluents, and at the same time it is economically feasible and environmentally friendly material which can be employed successfully for separation of Cu (II) on industrial scale.

ACKNOWLEDGEMENT

This research was supported by Research Grant (UMRG 056-09SUS) of University Malaya, Malaysia.

REFERENCES

1. Y. Jonathan, *Am. J. Appl. Sci.*, **7**(2), 153 (2010).
2. M. C. and B. Y. Kamruzzaman, *Am. J. Appl. Sci.*, **6**(7), 1418 (2009).
3. S. E. Bailey, T. J. Olin, R. M. Bricka and D. D. Adrian, *Water Res.*, **33**(11), 2469 (1999).
4. T. W. Tee and A. R. M. Khan, *Environ. Technol. Lett.*, **9**, 1223 (1988).
5. S. Cay, A. Uyanik and A. Ozajik, *Sep. Purif. Technol.*, **38**, 273 (2004).
6. L. Panda, B. Das and D. S. Rao, *Korean J. Chem. Eng.*, **28**(10), 2024 (2011).
7. K. S. Rao, S. Anand and P. Venkateswarlu, *Korean J. Chem. Eng.*, **27**(5), 1547 (2010).
8. C. Jeon, J. Y. Park and Y. J. Yoo, *Korean J. Chem. Eng.*, **18**(6), 955 (2001).
9. A. Pandey, A. Shukla and L. Ray, *Am. J. Biochem. Biotechnol.*, **3**(2), 55 (2009).
10. S. A. Dastgheib and A. D. Rockstraw, *Carbon*, **31**, 1849 (2001).
11. M. A. Hashim and K. H. Chu, *Chem. Eng. J.*, **97**, 249 (2004).
12. M. Horsfall, A. A. Abia and A. I. Spiff, *Afr. J. Biotechnol.*, **2**(10), 360 (2003).
13. A. Zuorro and R. Lavecchia, *Am. J. Appl. Sci.*, **7**, 153 (2010).
14. I. Villaescusa, N. Fiol, M. Martinez, N. Mirralles and J. Poch, *Water Res.*, **38**, 992 (2004).
15. A. Saeed, M. Iqbal and M. V. Akhtar, *J. Hazard. Mater.*, **B117**, 65 (2005).
16. I. Villaescusa, N. Fiol, M. Martinez, N. Mirralles and J. Poch, *Sep. Purif. Technol.*, **50**, 132 (2006).

17. A. Lopez-Delgado, C. Perez and F. A. Lopez, *Water Res.*, **32**, 989 (1998).
18. S. C. Pan, C. C. Lin and D. H. Tseng, *Resour. Conserv. Recycl.*, **39**, 79 (2003).
19. N. Calace, E. Nardi, B. M. Petronio, M. Pietroletti and G. Tosti, *Chemosphere*, **51**, 797 (1997).
20. R. Gundogan, B. Acemioglua and M. H. Alma, *J. Colloid Interface Sci.*, **269**, 303 (2004).
21. M. Goyal, V. K. Rattan, D. Aggarwal and R. C. Bansal, *Colloids Surf.*, **190**, 229 (2001).
22. L. Monser and N. Adhoum, *Sep. Purif. Technol.*, **26**, 137 (2002).
23. Z. Z. Chowdhury, S. M. Zain, A. K. Rashid and A. A. Ahmed, *Am. J. Appl. Sci.*, **8**(3), 230 (2011).
24. S. Aber, A. Khataee and M. Sheydaei, *Bioresour. Technol.*, **100**, 6586 (2009).
25. N. H. Phan, S. Rio, C. Faur, L. Le Coq, P. Le Cloirec and T. H. Nguyen, *Carbon*, **44**, 2569 (2006).
26. A. C Lua and T. Yang, *J. Colloid Interface Sci.*, **274**, 594 (2004).
27. IUPAC, IUPAC Manual of Symbols and Terminology, *Pure Appl. Chem*. 31:587 (1972).
28. V. C. Srivastava, I. D. Mall and I. M. Mishra, *Colloids and Surfaces A: Physiochem. Eng. Aspects.*, **312**, 172 (2008).
29. P. C. Heimenz and R. Razagopalan, Principles of Colloid and Surface Chemistry, 3rd Ed., Marcel Decker, New York, 516 (1977).
30. A. Habib, N. Islam, A. Islam and A. M. S. Alam, *Pak. J. Anal. Environ. Chem.*, **8**(1-2), 21 (2007).
31. S. Ong, P. Keng, A. Chong, S. Lee and Y. Hung, *Am. J. Environ. Sci.*, **6**(3), 244 (2010).
32. Y. S. Ho and G. McKay, *Process Biochemistry*, **34**(5), 451 (1999).
33. Y. S. Ho and G. McKay, *Water Res.*, **33**(2), 578 (1999).
34. W. J. Weber and J. C. Morris, *J. Sanit. Eng. Div. Am. Soc. Civ. Eng.*, **89**, 31 (1963).
35. M. Ozacar and I. A. Sengil, *Process Biochem.*, **40**, 565 (2005).
36. Y. S. Ho and G. McKay, *Can. J. Chem. Eng.*, **76**, 822 (1998).
37. M. H. Kalavathy, T. Karthikeyan, S. Rajgopal and L. R. Miranda, *J. Colloid Interface Sci.*, **292**, 354 (2005).
38. I. Langmuir, *J. Am. Chem. Soc.*, **38**, 2221 (1916).
39. H. M. F. Freundlich, *J. Phys. Chem.*, **57A**, 385 (1906).
40. M. I. Temkin and V. Pyzhev, *J. Phys. Chem. (U.S.S.R.)*, **13**, 851 (1939).
41. P. Pruksathorn and T. Vitidsant, *Am. J. Eng. Appl. Sci.*, **2**(1), 1 (2009).
42. M. Kazmi, N. Feroze, S. Naveed and S. H. Javed, *Korean J. Chem. Eng.*, **28**(10), 2033 (2011).
43. Z. Z. Chowdhury, S. M. Zain and A. K. Rashid, *E. J. Chem.*, **8**(1), 333 (2011).
44. M. Torab-Mostaidi, H. Ghassabzadeh, M. G. Maragheh, S. J. Ahmadi and H. Tahiri, *Braz. J. Chem. Eng.*, **27**(2), 299 (2010).
45. T. A. Kurniawan, G. Y. S. Chan, W. Lo and S. Babel, *Sci. Total Environ.*, **366**, 409 (2006).